Available online at www.sciencedirect.com
SCIENCE DIRECT
Journal of Sound and Vibration 294 (2006) 205–220
JOURNAL OF SOUND AND VIBRATION
www.elsevier.com/locate/jsvi

Finite element analysis of the vibrations of waveguides and periodic structures

D. Duhamel[a,*], B.R. Mace[b], M.J. Brennan[b]

[a]*LAMI - unité mixte ENPC/LCPC, Institut Navier, 6 et 8 Avenue Blaise Pascal, Cité Descartes, Champs sur Marne, 77455 Marne la Vallée, Cedex 2, France*

[b]*Institute of Sound and Vibration Research, University of Southampton, University Road, Highfield, Southampton S017 1BJ, UK*

Received 31 August 2004; received in revised form 18 October 2005; accepted 4 November 2005
Available online 18 January 2006

Abstract

Many structural components can be regarded as waveguides. They are uniform in one direction so that the cross section of the waveguide has the same physical and geometric properties at all points along the axis of the waveguide. In this paper a method is presented to calculate the forced response of such a structure using a combination of wave and finite element (FE) approaches. The method involves post-processing a conventional, but low order, FE model in which the mass and stiffness matrices are typically found using a conventional FE package. A section of the waveguide is meshed and the eigenvalues and eigenvectors of the resulting transfer matrix found. The eigenvectors form a set of basis functions for the analysis of the structure as a whole, allowing the global dynamic stiffness matrix to be built easily and then the forced response to be calculated very efficiently. The main advantage of the approach over the alternative waveguide/FE approach often termed the spectral FE method, is that conventional FE packages can be used to form the stiffness and mass matrices so that structures with complex geometries or material distributions can be analysed with relative ease. To demonstrate the efficacy of the method examples of the forced response for a finite beam and plate-strip are presented.

1. Introduction

Many structures have symmetry in one direction. As shown in Fig. 1, this symmetry can be a translation according to a privileged direction (a), a rotational symmetry (b) or a periodicity (c). Structures of this type can be considered as a waveguide. To predict their dynamic behaviour, for instance the calculation of a frequency response function (FRF), classical finite element (FE) software often offers no other choice than meshing the whole structure. Exceptions are rotational and cyclic symmetries, which are solved by a decomposition of the displacements in cosine and sine functions. A review of the current practises for these structures can be found in Ref. [1]. However, a better use of the symmetry could lead to a more efficient computation. Concerning the general calculation of waveguides, two approaches were mainly used in the past. A first group of authors consider uniform waveguides corresponding to cases (a) and (b) of Fig. 1, while the

*Corresponding author. Tel.: +33 1 64 15 37 28; fax: +33 1 64 15 37 41.
E-mail address: duhamel@lami.enpc.fr (D. Duhamel).

0022-460X/$ - see front matter © 2005 Elsevier Ltd. All rights reserved.
doi:10.1016/j.jsv.2005.11.014

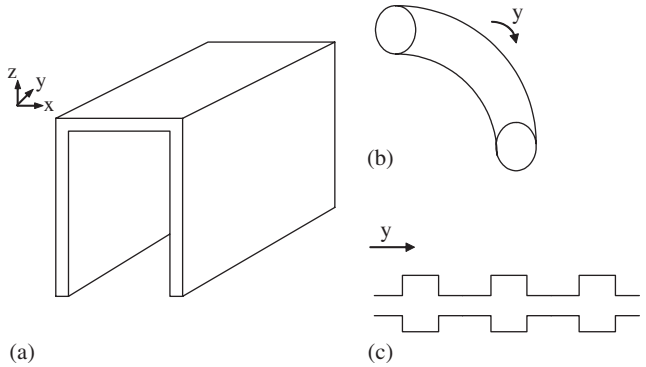

Fig. 1. Different structures with symmetries along the y direction: structures with: (a) translational symmetry; (b) rotational symmetry; (c) periodicity.

other group is interested by periodic structures, case (c) of Fig. 1. The case of periodic structures is clearly more general as uniform waveguides are only special cases of periodic structures with an arbitrary period.

The vibration of uniform waveguides has been the topic of much research. Von Flotow [2] and Beale and Accorsi [3] used the wave approach to study the vibration of structural networks composed of simple uniform beams, and solved for the dynamics of individual elements and of the junctions between elements by analytical methods. They described the dynamic behaviour of the structure in terms of the waves in each element, and the properties of the junctions between each element and the boundary conditions. The efficiency is greatly improved compared to FE methods as a beam can be modelled using only a single element. More recently the analysis of structures with constant cross section is made by the so-called spectral finite element (SFE) approach which was developed mainly by Finnveden [4,5]. The SFE considers more general uniform waveguides with a complex cross section. The displacements in the cross section can be described by the FE method while the variation along the axis of symmetry is expressed as an ordinary differential equation whose solution can be written in the form $e^{jky}U(x,z)$ where y is the direction of symmetry and x and z the coordinates of the cross section. Nilsson [6] has used the SFE approach to study structures made of plates and shells. Shorter [7] developed SFEs for viscoelastic laminates using Lagrange's equations, and found dispersion relations. Birgersson [8–10] used the SFE to solve various problems including plane waves and fluid structure interactions. Gry [11] applied similar ideas to the calculation of wave propagation in rails using a FE model of the cross section of a rail. He then calculated dispersion relations and accelerances. In the SFE, Finnveden [4,5] showed that the discrete FE equation can be written as

$$\left[\sum_{i=1}^{i=N} k^i \mathbf{K}_i - \omega^2 \mathbf{M}\right] \mathbf{U} = 0, \tag{1}$$

where $\mathbf{M}$ is the usual mass matrix. The stiffness matrix is developed for various powers of the wavenumber k^i, describing the propagation in the direction of symmetry. The stiffness matrices $\mathbf{K}_i$ are not standard matrices of the FE formulation and so must be determined for each problem with methods such as Lagrange's equations, Hamilton's principle or the virtual work principle. So for each type of element a complete analysis is needed, which starts by the development of special elements allowing the calculation of $\mathbf{K}_i$. This makes the connection with the standard use of the FE method difficult and does not allow the benefits of powerful existing FE software to be exploited. On the contrary the method proposed in this article can use the full set of elements found in existing FE software.

The second approach considers the propagation of waves in periodic structures and has also been studied extensively, see for instance the work of Brillouin [12] and the review paper by Mead [13]. The work has involved classical analysis of periodic structures. The approach is based on Floquet's principle or the transfer matrix. The basic idea is that the propagation of waves in a periodic structure can be obtained from propagation constants λ, which depend on the frequency, or by the transfer matrix $\mathbf{T}$, which relates the

displacements $\mathbf{q}$ and the forces $\mathbf{f}$ on both sides of the periodic element by the relationship

$$\begin{bmatrix} \mathbf{q}_R \\ -\mathbf{f}_R \end{bmatrix} = \mathbf{T} \begin{bmatrix} \mathbf{q}_L \\ \mathbf{f}_L \end{bmatrix} = \lambda \begin{bmatrix} \mathbf{q}_L \\ \mathbf{f}_L \end{bmatrix}, \tag{2}$$

where the subscripts L and R denote the left- and right-hand sides of the periodic element, respectively. Mead presented a general theory for wave propagation in periodic systems in Refs. [14–16]. He showed that the number of waves is twice the minimum number of degrees of freedom at coupling interfaces and can be decomposed into an equal number of positive and negative-going waves. The propagation constants λ are the eigenvalues of a transfer matrix $\mathbf{T}$ and can be written as $\lambda = e^{jkl}$ where l is the length of the periodic cell, k is a wavenumber and j the imaginary unit. For complex structures, FE models were used to calculate the propagation constants and wave modes. The main purpose is to get dispersion relations and to use them in energetic methods. Such ideas were developed by Houillon et al. in Refs. [17,18] and by Mace et al. in Refs. [19,20]. In Mace et al. an approach similar to the method developed in this paper was used to calculate dispersion relations but not for point force responses which is the subject of this paper. Bocquillet [21] applied similar ideas mainly also for energetic methods.

This paper presents a method, based on previous approaches to the analysis of periodic structures, to calculate the forced response of structures such as those illustrated in Fig. 1. This alternative approach is called the waveguide FE (WFE). A section of the waveguide, typically, but not necessarily, one element long, is modelled using conventional FE methods, using a commercial FE package. The resulting mass, stiffness and damping matrices are then post-processed to give the dynamic stiffness matrix of the cell. This is then reformulated in terms of waves, and periodic structure theory is used to build the dynamic stiffness matrix of the whole structure. An explicit, simple and stable expression for the global dynamic stiffness matrix is obtained from the wave shapes. It involves only propagation constants with modulus less than 1 which avoids most of the numerical problems found elsewhere. Then the response of the whole structure to harmonic excitation can be calculated easily by using the precedent dynamic stiffness matrix as a superelement.

The WFE approach is similar to the SFE approach, except that conventional FE software packages can be used for the modelling and that the dynamic stiffness matrix of the whole structure is built explicitly. This means that structures with complex geometries or material distributions can be analysed with relative ease. Compared with the standard FE approach, where the whole waveguide is meshed, the computational cost of the WFE approach is very low, because only a small section of the waveguide has to be meshed. Similar ideas were given by Ettouney [22] and also mainly in term of waves by Houillon [18] and Bocquillet [21] but no simple, neither numerically stable expression for the global stiffness matrix of the structure were provided by these authors. Gry and Gontier also extended their precedent work in Ref. [23] to take into account the periodic structure of the track by solving the problem using a transfer matrix approach. Here the dynamic stiffness matrix of the complete structure is built easily from the knowledge of wave modes and propagation constants calculated from one cell.

With the usual FE methods, it is well known that an increase in the frequency of analysis requires the mesh size to be decreased, and a common criterion is to have between 5 and 10 nodes per wavelength. Of course, this requirement can lead to large meshes and thus a heavy computational burden. Some methods such as the Guyan reduction described in Ref. [24] or [26] can be used to reduce the number of degrees of freedom. It consists in neglecting the inertia of slave degrees of freedom and in keeping a reduced dynamic system with only master degrees of freedom. However, it requires a judicious selection of these master degrees of freedom and leads anyway to an approximate system. In the WFE approach the solution is the same as one obtained with the usual FE method with a large number of cells and moreover the computation time is virtually independent of the number of cells in the structures. This means a much larger number of cells can be used leading to efficient computation for high frequencies. Further improvement can be achieved using a reduced wave basis to describe the displacements in a cross section. The number of degrees of freedom in a cross section can thus be greatly reduced, reducing computation time. The usual constraints are placed on the size of the mesh over the cross section, but the dimensionality of the problem is reduced.

The paper is organised as follows. Following the introduction, the FE analysis of periodic structures is presented. Then the general methodology for the analysis of wave propagation in periodic structures is given

in Section 3. A reduced basis is described. In Section 4 this is used to calculate the main result of the paper which is the expression of the dynamic stiffness matrix of a complete structure. Two examples including a beam and a plate are described in Section 5 before the paper is closed with some general conclusions.

2. Finite element analysis of periodic structures

2.1. Cell dynamics

A section of the structure considered is shown schematically in Fig. 2. The section is divided into a finite number of cells with index n. The cells are meshed with an equal number of nodes on their left- and right-hand edges. The discrete dynamic equation of a cell obtained from the FE model at a frequency ω is given by

$$(\mathbf{K} + \mathrm{j}\omega\mathbf{C} - \omega^2\mathbf{M})\,\mathbf{q} = \mathbf{f}, \tag{3}$$

where $\mathbf{K}$, $\mathbf{M}$, and $\mathbf{C}$ are the stiffness, mass and damping matrices, respectively, $\mathbf{f}$ is the loading vector and $\mathbf{q}$ the vector of the degrees of freedom. Introducing the dynamic stiffness matrix $\tilde{\mathbf{D}} = \mathbf{K} + \mathrm{j}\omega\mathbf{C} - \omega^2\mathbf{M}$, decomposing into left (L) and right (R) boundaries, and interior (I) degrees of freedom, and assuming that there are no external forces on the interior nodes, results in the following matrix equation:

$$\begin{bmatrix} \tilde{\mathbf{D}}_{II} & \tilde{\mathbf{D}}_{IL} & \tilde{\mathbf{D}}_{IR} \\ \tilde{\mathbf{D}}_{LI} & \tilde{\mathbf{D}}_{LL} & \tilde{\mathbf{D}}_{LR} \\ \tilde{\mathbf{D}}_{RI} & \tilde{\mathbf{D}}_{RL} & \tilde{\mathbf{D}}_{RR} \end{bmatrix} \begin{bmatrix} \mathbf{q}_I \\ \mathbf{q}_L \\ \mathbf{q}_R \end{bmatrix} = \begin{bmatrix} \mathbf{0} \\ \mathbf{f}_L \\ \mathbf{f}_R \end{bmatrix}. \tag{4}$$

The interior degrees of freedom can be eliminated using the first row of Eq. (4), which results in

$$\mathbf{q}_I = -\tilde{\mathbf{D}}_{II}^{-1}(\tilde{\mathbf{D}}_{IL}\mathbf{q}_L + \tilde{\mathbf{D}}_{IR}\mathbf{q}_R). \tag{5}$$

This leads to

$$\begin{bmatrix} \tilde{\mathbf{D}}_{LL} - \tilde{\mathbf{D}}_{LI}\tilde{\mathbf{D}}_{II}^{-1}\tilde{\mathbf{D}}_{IL} & \tilde{\mathbf{D}}_{LR} - \tilde{\mathbf{D}}_{LI}\tilde{\mathbf{D}}_{II}^{-1}\tilde{\mathbf{D}}_{IR} \\ \tilde{\mathbf{D}}_{RL} - \tilde{\mathbf{D}}_{RI}\tilde{\mathbf{D}}_{II}^{-1}\tilde{\mathbf{D}}_{IL} & \tilde{\mathbf{D}}_{RR} - \tilde{\mathbf{D}}_{RI}\tilde{\mathbf{D}}_{II}^{-1}\tilde{\mathbf{D}}_{IR} \end{bmatrix} \begin{bmatrix} \mathbf{q}_L \\ \mathbf{q}_R \end{bmatrix} = \begin{bmatrix} \mathbf{f}_L \\ \mathbf{f}_R \end{bmatrix}, \tag{6}$$

which can be written as

$$\begin{bmatrix} \mathbf{D}_{LL} & \mathbf{D}_{LR} \\ \mathbf{D}_{RL} & \mathbf{D}_{RR} \end{bmatrix} \begin{bmatrix} \mathbf{q}_L \\ \mathbf{q}_R \end{bmatrix} = \begin{bmatrix} \mathbf{f}_L \\ \mathbf{f}_R \end{bmatrix}. \tag{7}$$

The new dynamic stiffness matrix is thus obtained after elimination of the interior degrees of freedom. By symmetry of the stiffness, damping and mass matrices, the dynamic stiffness matrix is also symmetric, which leads to ${}^{\mathrm{t}}\mathbf{D}_{LL} = \mathbf{D}_{LL}$, ${}^{\mathrm{t}}\mathbf{D}_{RR} = \mathbf{D}_{RR}$ and ${}^{\mathrm{t}}\mathbf{D}_{LR} = \mathbf{D}_{RL}$, where the superscript t indicates the transpose. Eq. (7), which relates the forces and displacements on the two sides of the cell, is the starting point for the WFE analysis.

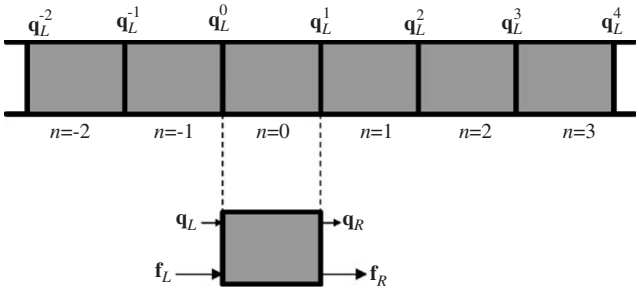

Fig. 2. Structure with periodic elements. A cell is shown with the force and displacement vectors on the right and left-hand sides.

2.2. Reduced basis

The dynamic stiffness matrix introduced in Eq. (7) can be used when the number of degrees of freedom is small. For a large number of degrees of freedom, it is better to introduce a reduced basis and a smaller number of parameters describing the displacements in the cross section. Introducing independent basis functions $\mathbf{Q}_i, 1 \leqslant i \leqslant N_s$ in a cross section with N_s degrees of freedom, the displacement can be written as

$$\mathbf{q} = \sum_{i=1}^{i=N_s} r_i \mathbf{Q}_i. \tag{8}$$

If we retain only n functions in the sum, with $n < N_s$, the displacement in a cross section can be approximated by

$$\mathbf{q} \cong \sum_{i=1}^{i=n} r_i \mathbf{Q}_i. \tag{9}$$

The quality of the approximation depends on the choice of the basis $\mathbf{Q}_i$ and the number of retained basis functions n, which ideally should be much smaller than N_s. Introducing the matrix

$$\mathbf{Q}^+ = [\mathbf{Q}_1, \ldots, \mathbf{Q}_n]. \tag{10}$$

The reduced dynamic stiffness matrix can be defined by

$$\begin{bmatrix} \mathbf{D}^r_{LL} & \mathbf{D}^r_{LR} \\ \mathbf{D}^r_{RL} & \mathbf{D}^r_{RR} \end{bmatrix} \begin{bmatrix} \mathbf{r}_L \\ \mathbf{r}_R \end{bmatrix} = \begin{bmatrix} \mathbf{g}_L \\ \mathbf{g}_R \end{bmatrix}, \tag{11}$$

with the projections of the dynamic stiffness matrices on the new basis defined by

$$\begin{aligned} \mathbf{D}^r_{LL} &= {}^t\mathbf{Q}^+ \mathbf{D}_{LL} \mathbf{Q}^+, \\ \mathbf{D}^r_{LR} &= {}^t\mathbf{Q}^+ \mathbf{D}_{LR} \mathbf{Q}^+, \\ \mathbf{D}^r_{RL} &= {}^t\mathbf{Q}^+ \mathbf{D}_{RL} \mathbf{Q}^+, \\ \mathbf{D}^r_{RR} &= {}^t\mathbf{Q}^+ \mathbf{D}_{RR} \mathbf{Q}^+ \end{aligned} \tag{12}$$

and the reduced forces given by

$$\begin{aligned} \mathbf{g}_L &= {}^t\mathbf{Q}^+ \mathbf{f}_L = {}^t[g_{L1} \cdots g_{Ln}], \\ \mathbf{g}_R &= {}^t\mathbf{Q}^+ \mathbf{f}_R = {}^t[g_{R1} \cdots g_{Rn}]. \end{aligned} \tag{13}$$

Thus in the reduced basis coordinates the behaviour of the cell is described by Eq. (11) which is similar to Eq. (7). Therefore, the same approach can be used for structures described by the physical degrees of freedom as in Eq. (7) or by another basis as in Eq. (11). Henceforth, no distinction is made between these two relationships and the vector $\mathbf{q}_L$ equally describes either the physical degrees of freedom or the reduced basis form. The question then remains as to how to find a good basis such that Eq. (11) is a smaller system of equations than Eq. (7). This is addressed later in the paper.

3. Wave analysis in a cell

3.1. Transfer matrix

Consider the structure shown in Fig. 2. If there are no external forces applied to the structure, continuity of displacements and equilibrium of forces at the boundary between cells n and $n+1$ yields,

$$\begin{aligned} \mathbf{q}^{n+1}_L &= \mathbf{q}^n_R, \\ \mathbf{f}^{n+1}_L &= -\mathbf{f}^n_R. \end{aligned} \tag{14}$$

The transfer matrix $\mathbf{T}$ links the displacements and forces in cross sections n and $n+1$ as follows:

$$\mathbf{T}\begin{bmatrix}\mathbf{q}_L^n\\ \mathbf{f}_L^n\end{bmatrix}=\begin{bmatrix}\mathbf{q}_R^n\\ -\mathbf{f}_R^n\end{bmatrix}=\begin{bmatrix}\mathbf{q}_L^{n+1}\\ \mathbf{f}_L^{n+1}\end{bmatrix}. \tag{15}$$

Combining Eqs. (7), (14) and (15) the transfer matrix can be written in terms of the dynamic stiffness matrix as

$$\mathbf{T}=\begin{bmatrix}-\mathbf{D}_{LR}^{-1}\mathbf{D}_{LL} & \mathbf{D}_{LR}^{-1}\\ -\mathbf{D}_{RL}+\mathbf{D}_{RR}\mathbf{D}_{LR}^{-1}\mathbf{D}_{LL} & -\mathbf{D}_{RR}\mathbf{D}_{LR}^{-1}\end{bmatrix}. \tag{16}$$

Free wave propagation is described by the eigenproblem

$$\mathbf{T}\begin{bmatrix}\mathbf{q}_L\\ \mathbf{f}_L\end{bmatrix}=\lambda\begin{bmatrix}\mathbf{q}_L\\ \mathbf{f}_L\end{bmatrix}. \tag{17}$$

The eigenvector associated with the eigenvalue λ_i is denoted by

$$\mathbf{\Phi}_i=\begin{bmatrix}\mathbf{q}(\lambda_i)\\ \mathbf{f}(\lambda_i)\end{bmatrix} \tag{18}$$

and is termed a basis wave vector.

3.2. Properties of wave vectors

The first row of Eq. (17) leads to

$$(\mathbf{D}_{LL}+\lambda\mathbf{D}_{LR})\mathbf{q}_L=\mathbf{f}_L. \tag{19}$$

Combining this with the second row of Eq. (17) gives

$$\left(\mathbf{D}_{LL}+\mathbf{D}_{RR}+\lambda\mathbf{D}_{LR}+\frac{1}{\lambda}\mathbf{D}_{RL}\right)\mathbf{q}_L=0. \tag{20}$$

The eigenvector $\mathbf{q}_L$ is thus the solution of a quadratic eigenvalue problem. Taking the transpose of Eq. (20) gives

$${}^{\mathrm{t}}\mathbf{q}_{\mathbf{L}}\left(\mathbf{D}_{LL}+\mathbf{D}_{RR}+\lambda\mathbf{D}_{RL}+\frac{1}{\lambda}\mathbf{D}_{LR}\right)=0, \tag{21}$$

where the symmetry of the dynamic stiffness matrix has been used. Thus $\mathbf{q}_L$ is both a right-eigenvector associated with the eigenvalue λ and a left-eigenvector associated with the eigenvalue $1/\lambda$. Since the left and right eigenproblems have identical eigenvalues, it follows that if λ is an eigenvalue of Eq. (20) then so, too, is $1/\lambda$. These represent a pair of positive- and negative-going waves. This is true for any shape or property of the cell. The right eigenvector of Eq. (17) for eigenvalue λ_i is given by

$$\mathbf{\Phi}_i=\begin{bmatrix}\mathbf{q}(\lambda_i)\\ (\mathbf{D}_{LL}+\lambda_i\mathbf{D}_{LR})\mathbf{q}(\lambda_i)\end{bmatrix} \tag{22}$$

and the left eigenvector associated with λ_i is given by

$$\mathbf{\Psi}_i=\begin{bmatrix}{}^{\mathrm{t}}\mathbf{q}\left(\frac{1}{\lambda_i}\right)(\mathbf{D}_{RR}+\lambda_i\mathbf{D}_{LR}) & {}^{\mathrm{t}}\mathbf{q}\left(\frac{1}{\lambda_i}\right)\end{bmatrix}. \tag{23}$$

Orthogonality properties can be obtained from the relationships

$$\begin{aligned}\mathbf{T}\mathbf{\Phi}_j&=\lambda_j\mathbf{\Phi}_j,\\ \mathbf{\Psi}_i\mathbf{T}&=\lambda_i\mathbf{\Psi}_i,\end{aligned} \tag{24}$$

which leads to

$$\mathbf{\Psi}_i \mathbf{T} \mathbf{\Phi}_j = \lambda_j \mathbf{\Psi}_i \mathbf{\Phi}_j = \lambda_i \mathbf{\Psi}_i \mathbf{\Phi}_j. \tag{25}$$

This quantity must equal zero if $\lambda_i \neq \lambda_j$, so, the left and right eigenvectors are such that

$$\mathbf{\Psi}_i \mathbf{\Phi}_j = d_i \delta_{ij}, \tag{26}$$

where d_i is some constant. A normalisation of the eigenvectors could be chosen so that $d_i = 1$, but here the vectors $\mathbf{q}(\lambda_i)$ are normalised instead.

3.3. Wave decomposition in a cell

From the preceding section, it is clear that the $2n$ eigenvalues of Eq. (17) can be split into two sets of n eigenvalues and eigenvectors which are denoted by $(\lambda_i, \mathbf{\Phi}_i^+)$ and $(1/\lambda_i, \mathbf{\Phi}_i^-)$, with the first set such that $|\lambda_i| \leqslant 1$. In the case $|\lambda_i| = 1$, the first set must contain the waves propagating in the positive direction, which are such that $\mathrm{Re}\{\mathrm{j}\omega \mathbf{q}_L^H \mathbf{f}_L\} < 0$. The inverse eigenvalue $1/\lambda_i$, in the second set, is associated with the waves such that $\mathrm{Re}\{\mathrm{j}\omega \mathbf{q}_L^H \mathbf{f}_L\} > 0$. It has been shown by Mead [16] that for symmetric elements and attenuating waves, the positive and negative eigenvectors are equal, that is $\mathbf{q}(\lambda_i) = \mathbf{q}(1/\lambda_i)$ provided that λ_i and $\mathbf{T}$ are real. In the general case there is no simple relationship between these two vectors.

These waves are now used as a basis in a cross section. The left state vector is given by the following sum of positive and negative-going waves with respective amplitudes a_i^+ and a_i^-:

$$\mathbf{x}_L = \begin{bmatrix} \mathbf{q}_L \\ \mathbf{f}_L \end{bmatrix} = \sum_{i=1}^{i=n} (a_i^+ \mathbf{\Phi}_i^+ + a_i^- \mathbf{\Phi}_i^-). \tag{27}$$

In the same way, the right state vector is given by

$$\mathbf{x}_R = \begin{bmatrix} \mathbf{q}_R \\ -\mathbf{f}_R \end{bmatrix} = \sum_{i=1}^{i=n} (b_i^+ \mathbf{\Phi}_i^+ + b_i^- \mathbf{\Phi}_i^-). \tag{28}$$

The relationships between the incoming and outgoing waves in the cell are obtained from the relation $\mathbf{x}_R = \mathbf{T}\mathbf{x}_L$. Because the vectors $\mathbf{\Phi}_i^+$ and $\mathbf{\Phi}_i^-$ are eigenvectors of $\mathbf{T}$, this relationship can be written as

$$\begin{bmatrix} \mathbf{b}^+ \\ \mathbf{a}^- \end{bmatrix} = \begin{bmatrix} \mathbf{\Lambda} & 0 \\ 0 & \mathbf{\Lambda} \end{bmatrix} \begin{bmatrix} \mathbf{a}^+ \\ \mathbf{b}^- \end{bmatrix}, \tag{29}$$

where the vectors $\mathbf{a}^+, \mathbf{a}^-, \mathbf{b}^+$ and $\mathbf{b}^-$ are the vectors of wave amplitudes and the diagonal matrix $\mathbf{\Lambda} = \mathrm{diag}(\lambda_1, \ldots, \lambda_n)$ contains the eigenvalues of modulus less than or equal to one.

3.4. Calculation of the reduced basis

When the number of degrees of freedom in a cross section is large, it is better to use a reduced basis as discussed in Section 2.2. A possible choice for the basis $\mathbf{Q}_i, 1 \leqslant i \leqslant N_s$ in a cross section is given here. One possibility is to use the eigenvectors $\mathbf{q}(\lambda_i)$ for a specified frequency, for instance the highest frequency $f_{\max}$ used in the analysis, and to select a limited number of vectors, those whose eigenvalues are close to one. These would typically include all the propagating wave components, for which $|\lambda_i| = 1$, together with the least-rapidly attenuating waves, i.e. those for which $|\lambda_i| < 1$ is largest. To calculate the eigenvalues and eigenvectors numerically, one has to solve the eigenvalue problem (17) or (20). For a large number of degrees of freedom, direct use of usual numerical solvers can lead to difficulties because the transfer matrix may be ill-conditioned. It is better, for instance, to define a problem in term of the eigenvalue $(\lambda + 1/\lambda)$ as proposed by Gry and Gontier in Ref. [22] or Zhong [25], who showed that the transfer matrix is symplectic and gave a detailed analysis of its eigenvectors. This means that we search for the eigenvalues of $\mathbf{T} + \mathbf{T}^{-1}$ instead of the

eigenvalues of $\mathbf{T}$. The eigenvalue problem in Eq. (20) can be reformulated as

$$\begin{bmatrix} \mathbf{O} & \mathbf{D}_{RL} \\ -\mathbf{D}_{RL} & -\mathbf{D}_{LL}-\mathbf{D}_{RR} \end{bmatrix} \begin{bmatrix} \mathbf{q}_L \\ \tilde{\mathbf{q}}_L \end{bmatrix} = \lambda \begin{bmatrix} \mathbf{D}_{RL} & \mathbf{O} \\ \mathbf{O} & \mathbf{D}_{LR} \end{bmatrix} \begin{bmatrix} \mathbf{q}_L \\ \tilde{\mathbf{q}}_L \end{bmatrix}, \tag{30}$$

with $\tilde{\mathbf{q}}_L = \lambda \mathbf{q}_L$. Another possibility is in the form

$$\begin{bmatrix} -\mathbf{D}_{LL}-\mathbf{D}_{RR} & -\mathbf{D}_{LR} \\ \mathbf{D}_{LR} & \mathbf{O} \end{bmatrix} \begin{bmatrix} \mathbf{q}_L \\ \tilde{\mathbf{q}}_L \end{bmatrix} = \frac{1}{\lambda} \begin{bmatrix} \mathbf{D}_{RL} & \mathbf{O} \\ \mathbf{O} & \mathbf{D}_{LR} \end{bmatrix} \begin{bmatrix} \mathbf{q}_L \\ \tilde{\mathbf{q}}_L \end{bmatrix}. \tag{31}$$

Taking the sum of Eqs. (30) and (31) and reorganising leads to

$$\begin{bmatrix} \mathbf{D}_{RL} & \mathbf{O} \\ \mathbf{O} & \mathbf{D}_{LR} \end{bmatrix} \begin{bmatrix} \mathbf{q}_L \\ \tilde{\mathbf{q}}_L \end{bmatrix} = \frac{1}{\lambda + (1/\lambda)} \begin{bmatrix} -(\mathbf{D}_{LL}+\mathbf{D}_{RR}) & -(\mathbf{D}_{LR}-\mathbf{D}_{RL}) \\ (\mathbf{D}_{LR}-\mathbf{D}_{RL}) & -(\mathbf{D}_{LL}+\mathbf{D}_{RR}) \end{bmatrix} \begin{bmatrix} \mathbf{q}_L \\ \tilde{\mathbf{q}}_L \end{bmatrix}. \tag{32}$$

This last system has only double eigenvalues. Denoting two independent eigenvectors associated to the same eigenvalue as $\mathbf{w}_1$ and $\mathbf{w}_2$, an eigenvector of the system given by Eq. (30) associated with the eigenvalue λ can be decomposed as

$$\mathbf{w} = \alpha_1 \mathbf{w}_1 + \alpha_2 \mathbf{w}_2. \tag{33}$$

Inserting this into Eq. (30) gives

$$\begin{bmatrix} \lambda \mathbf{D}_{RL} & -\mathbf{D}_{RL} \\ \mathbf{D}_{RL} & \mathbf{D}_{LL}+\mathbf{D}_{RR}+\lambda \mathbf{D}_{LR} \end{bmatrix} (\alpha_1 \mathbf{w}_1 + \alpha_2 \mathbf{w}_2) = 0. \tag{34}$$

Taking, for instance, the scalar product with the vector $\mathbf{w}_1$, leads to a relationship between α_1 and α_2 which gives the vector $\mathbf{w}$ up to a normalisation factor. Now the eigenvectors obtained for the frequency $f_{\max}$ are used in Eq. (11) as basis vectors for all the frequencies. This means that the matrix $\mathbf{Q}^+$ defined in Eq. (10) is given by

$$\mathbf{Q}^+ = [q(\lambda_1), \ldots, q(\lambda_n)]. \tag{35}$$

The eigenvalues $\lambda_i, 1 \leqslant i \leqslant n$, are those whose moduli are closest to unity among the N_s eigenvalues of Eq. (17). Only these n eigenvalues are calculated. The number n of vectors to be retained will be shown in the examples given in Section 5. For some problems use of the same basis for all frequencies is not possible. If this is so a new basis must be calculated for a selected set of frequencies $(f_1, f_2, \ldots, f_n)$ in the frequency range of calculation. The basis calculated at the frequency f_i is used for frequencies near f_i.

4. Analysis of a complete structure

4.1. Dynamic stiffness matrix of a N-cell structure

Consider now the structure in Fig. 3, which is split into N identical cells. The objective is to calculate the dynamic stiffness matrix of this structure. This means that the relationship between the forces and displacements at each end of the structure needs to be determined. From Eqs. (27) and (28), and using the orthogonal properties given in Eq. (26), the wave amplitudes can be obtained from the left and right state

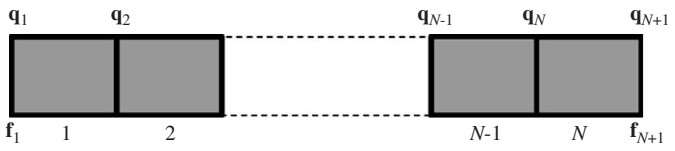

Fig. 3. Structure with N cells.

vectors by the scalar products

$$\begin{aligned} d_i^+ a_i^+ &= \boldsymbol{\Psi}_i^+ \cdot \mathbf{x}_L, \quad d_i^+ b_i^+ = \boldsymbol{\Psi}_i^+ \cdot \mathbf{x}_R, \\ d_i^- a_i^- &= \boldsymbol{\Psi}_i^- \cdot \mathbf{x}_L, \quad d_i^- b_i^- = \boldsymbol{\Psi}_i^- \cdot \mathbf{x}_R, \end{aligned} \tag{36}$$

where the $d_i^{\pm}$ are the factors given in Eq. (26). Thus Eq. (29) can be written as

$$\begin{bmatrix} \boldsymbol{\Psi}^+ \cdot \mathbf{x}_R \\ \boldsymbol{\Psi}^- \cdot \mathbf{x}_L \end{bmatrix} = \begin{bmatrix} \boldsymbol{\Lambda} & 0 \\ 0 & \boldsymbol{\Lambda} \end{bmatrix} \begin{bmatrix} \boldsymbol{\Psi}^+ \cdot \mathbf{x}_L \\ \boldsymbol{\Psi}^- \cdot \mathbf{x}_R \end{bmatrix}, \tag{37}$$

where $\boldsymbol{\Psi}^+$ and $\boldsymbol{\Psi}^-$ are matrices whose rows are the vectors $\boldsymbol{\Psi}_i^+$ and $\boldsymbol{\Psi}_i^-$, respectively.

Generalising Eq. (37) for the case of N cells gives

$$\begin{bmatrix} \boldsymbol{\Psi}^+ \cdot \mathbf{x}_{N+1} \\ \boldsymbol{\Psi}^- \cdot \mathbf{x}_1 \end{bmatrix} = \begin{bmatrix} \boldsymbol{\Lambda}^N & 0 \\ 0 & \boldsymbol{\Lambda}^N \end{bmatrix} \begin{bmatrix} \boldsymbol{\Psi}^+ \cdot \mathbf{x}_1 \\ \boldsymbol{\Psi}^- \cdot \mathbf{x}_{N+1} \end{bmatrix}, \tag{38}$$

where $\mathbf{x}_1$ is the left state vector comprising the displacements and forces in the first section (number 1) and $\mathbf{x}_{N+1}$ are the displacements and forces in the last section (number $N+1$). The matrices $\boldsymbol{\Psi}^+$ and $\boldsymbol{\Psi}^-$ can be partitioned as follows:

$$\boldsymbol{\Psi}^+ = [{}^{\mathrm{t}}\mathbf{F}^- \ {}^{\mathrm{t}}\mathbf{Q}^-], \quad \boldsymbol{\Psi}^- = [{}^{\mathrm{t}}\mathbf{F}^+ \ {}^{\mathrm{t}}\mathbf{Q}^+], \tag{39}$$

where

$$\begin{aligned} \mathbf{Q}^+ &= [\mathbf{q}(\lambda_1) \ \cdots \ q(\lambda_n)], \\ \mathbf{Q}^- &= \left[\mathbf{q}\left(\frac{1}{\lambda_1}\right) \ \cdots \ \mathbf{q}\left(\frac{1}{\lambda_n}\right)\right] \end{aligned} \tag{40}$$

and

$$\begin{aligned} {}^{\mathrm{t}}\mathbf{F}^+ &= {}^{\mathrm{t}}\mathbf{Q}^+\mathbf{D}_{RR} + \boldsymbol{\Lambda}^{-1}\,{}^{\mathrm{t}}\mathbf{Q}^+\mathbf{D}_{LR} = -{}^{\mathrm{t}}\mathbf{Q}^+\mathbf{D}_{LL} - \boldsymbol{\Lambda}\,{}^{\mathrm{t}}\mathbf{Q}^+\mathbf{D}_{RL}, \\ {}^{\mathrm{t}}\mathbf{F}^- &= {}^{\mathrm{t}}\mathbf{Q}^-\mathbf{D}_{RR} + \boldsymbol{\Lambda}\,{}^{\mathrm{t}}\mathbf{Q}^-\mathbf{D}_{LR} = -{}^{\mathrm{t}}\mathbf{Q}^-\mathbf{D}_{LL} - \boldsymbol{\Lambda}^{-1}\,{}^{\mathrm{t}}\mathbf{Q}^-\mathbf{D}_{RL}. \end{aligned} \tag{41}$$

The matrices $F^{\pm}$ in Eq. (41) are related to the force components of the left eigenvectors. Eq. (38) can also be written as

$$\begin{bmatrix} {}^{\mathrm{t}}\mathbf{F}^- & {}^{\mathrm{t}}\mathbf{Q}^- \\ \boldsymbol{\Lambda}^N\,{}^{\mathrm{t}}\mathbf{F}^+ & \boldsymbol{\Lambda}^N\,{}^{\mathrm{t}}\mathbf{Q}^+ \end{bmatrix} \begin{bmatrix} \mathbf{q}_{N+1} \\ -\mathbf{f}_{N+1} \end{bmatrix} = \begin{bmatrix} \boldsymbol{\Lambda}^N\,{}^{\mathrm{t}}\mathbf{F}^- & \boldsymbol{\Lambda}^N\,{}^{\mathrm{t}}\mathbf{Q}^- \\ {}^{\mathrm{t}}\mathbf{F}^+ & {}^{\mathrm{t}}\mathbf{Q}^+ \end{bmatrix} \begin{bmatrix} \mathbf{q}_1 \\ \mathbf{f}_1 \end{bmatrix} \tag{42}$$

or in the form

$$\begin{bmatrix} \boldsymbol{\Lambda}^N\,{}^{\mathrm{t}}\mathbf{Q}^- & {}^{\mathrm{t}}\mathbf{Q}^- \\ {}^{\mathrm{t}}\mathbf{Q}^+ & \boldsymbol{\Lambda}^N\,{}^{\mathrm{t}}\mathbf{Q}^+ \end{bmatrix} \begin{bmatrix} \mathbf{f}_1 \\ \mathbf{f}_{N+1} \end{bmatrix} = \begin{bmatrix} -\boldsymbol{\Lambda}^N\,{}^{\mathrm{t}}\mathbf{F}^- & {}^{\mathrm{t}}\mathbf{F}^- \\ -{}^{\mathrm{t}}\mathbf{F}^+ & \boldsymbol{\Lambda}^N\,{}^{\mathrm{t}}\mathbf{F}^+ \end{bmatrix} \begin{bmatrix} \mathbf{q}_1 \\ \mathbf{q}_{N+1} \end{bmatrix}. \tag{43}$$

Replacing $\mathbf{F}^{\pm}$ by the expressions given in Eq. (41) results in

$$\begin{aligned} &\begin{bmatrix} \boldsymbol{\Lambda}^N\,{}^{\mathrm{t}}\mathbf{Q}^- & {}^{\mathrm{t}}\mathbf{Q}^- \\ {}^{\mathrm{t}}\mathbf{Q}^+ & \boldsymbol{\Lambda}^N\,{}^{\mathrm{t}}\mathbf{Q}^+ \end{bmatrix} \begin{bmatrix} \mathbf{f}_1 \\ \mathbf{f}_{N+1} \end{bmatrix} \\ &= \begin{bmatrix} \boldsymbol{\Lambda}^N\,{}^{\mathrm{t}}\mathbf{Q}^-\mathbf{D}_{LL} + \boldsymbol{\Lambda}^{N-1}\,{}^{\mathrm{t}}\mathbf{Q}^-\mathbf{D}_{RL} & {}^{\mathrm{t}}\mathbf{Q}^-\mathbf{D}_{RR} + \boldsymbol{\Lambda}\,{}^{\mathrm{t}}\mathbf{Q}^-\mathbf{D}_{LR} \\ {}^{\mathrm{t}}\mathbf{Q}^+\mathbf{D}_{LL} + \boldsymbol{\Lambda}\,{}^{\mathrm{t}}\mathbf{Q}^+\mathbf{D}_{RL} & \boldsymbol{\Lambda}^N\,{}^{\mathrm{t}}\mathbf{Q}^+\mathbf{D}_{RR} + \boldsymbol{\Lambda}^{N-1}\,{}^{\mathrm{t}}\mathbf{Q}^+\mathbf{D}_{LR} \end{bmatrix} \begin{bmatrix} \mathbf{q}_1 \\ \mathbf{q}_{N+1} \end{bmatrix} \\ &= \begin{bmatrix} \boldsymbol{\Lambda}^N\,{}^{\mathrm{t}}\mathbf{Q}^- & {}^{\mathrm{t}}\mathbf{Q}^- \\ {}^{\mathrm{t}}\mathbf{Q}^+ & \boldsymbol{\Lambda}^N\,{}^{\mathrm{t}}\mathbf{Q}^+ \end{bmatrix} \begin{bmatrix} \mathbf{D}_{LL}\mathbf{q}_1 \\ \mathbf{D}_{RR}\mathbf{q}_{N+1} \end{bmatrix} + \begin{bmatrix} \boldsymbol{\Lambda}^{N-1}\,{}^{\mathrm{t}}\mathbf{Q}^- & \boldsymbol{\Lambda}\,{}^{\mathrm{t}}\mathbf{Q}^- \\ \boldsymbol{\Lambda}\,{}^{\mathrm{t}}\mathbf{Q}^+ & \boldsymbol{\Lambda}^{N-1}\,{}^{\mathrm{t}}\mathbf{Q}^+ \end{bmatrix} \begin{bmatrix} \mathbf{D}_{RL}\mathbf{q}_1 \\ \mathbf{D}_{LR}\mathbf{q}_{N+1} \end{bmatrix}. \end{aligned} \tag{44}$$

Multiplying by the inverse of the matrix on the left-hand side leads to

$$\begin{bmatrix} \mathbf{f}_1 \\ \mathbf{f}_{N+1} \end{bmatrix} = \begin{bmatrix} \mathbf{D}_{LL}\mathbf{q}_1 \\ \mathbf{D}_{RR}\mathbf{q}_{N+1} \end{bmatrix} + \begin{bmatrix} ({}^{t}\mathbf{Q}^{-})^{-1}\mathbf{\Lambda}^{N}\,{}^{t}\mathbf{Q}^{-} & \mathbf{I} \\ \mathbf{I} & ({}^{t}\mathbf{Q}^{+})^{-1}\mathbf{\Lambda}^{N}\,{}^{t}\mathbf{Q}^{+} \end{bmatrix}^{-1} \times \begin{bmatrix} ({}^{t}\mathbf{Q}^{-})^{-1}\mathbf{\Lambda}^{N-1}\,{}^{t}\mathbf{Q}^{-} & ({}^{t}\mathbf{Q}^{-})^{-1}\mathbf{\Lambda}\,{}^{t}\mathbf{Q}^{-} \\ ({}^{t}\mathbf{Q}^{+})^{-1}\mathbf{\Lambda}\,{}^{t}\mathbf{Q}^{+} & ({}^{t}\mathbf{Q}^{+})^{-1}\mathbf{\Lambda}^{N-1}\,{}^{t}\mathbf{Q}^{+} \end{bmatrix} \begin{bmatrix} \mathbf{D}_{RL}\mathbf{q}_1 \\ \mathbf{D}_{LR}\mathbf{q}_{N+1} \end{bmatrix}. \tag{45}$$

By using the symmetry of the cell dynamic stiffness matrix and the propagation matrices

$$\begin{aligned} \mathbf{P}_l &= \mathbf{Q}^{-}\mathbf{\Lambda}(\mathbf{Q}^{-})^{-1}, \\ \mathbf{P}_r &= \mathbf{Q}^{+}\mathbf{\Lambda}(\mathbf{Q}^{+})^{-1}, \end{aligned} \tag{46}$$

where $\mathbf{P}_r$ is the matrix of eigenvalues λ_i and eigenvectors $\mathbf{q}(\lambda_i)$, and $\mathbf{P}_l$ is the matrix of eigenvalues λ_i and eigenvectors $\mathbf{q}(1/\lambda_i)$, yields

$$\begin{bmatrix} \mathbf{f}_1 \\ \mathbf{f}_{N+1} \end{bmatrix} = \mathbf{D}_T \begin{bmatrix} \mathbf{q}_1 \\ \mathbf{q}_{N+1} \end{bmatrix}, \tag{47}$$

where $\mathbf{D}_T$ is the dynamic stiffness matrix of the whole structure given by

$$\mathbf{D}_T = \begin{bmatrix} \mathbf{D}_{LL} & 0 \\ 0 & \mathbf{D}_{RR} \end{bmatrix} + \begin{bmatrix} \mathbf{D}_{LR} & 0 \\ 0 & \mathbf{D}_{RL} \end{bmatrix} \begin{bmatrix} \mathbf{P}_l^{N-1} & \mathbf{P}_r \\ \mathbf{P}_l & \mathbf{P}_r^{N-1} \end{bmatrix} \begin{bmatrix} \mathbf{P}_l^{N} & \mathbf{I} \\ \mathbf{I} & \mathbf{P}_r^{N} \end{bmatrix}^{-1}. \tag{48}$$

This expression of the dynamic stiffness matrix is the central result of this paper. The dynamic stiffness matrix can easily be calculated when the propagation matrices $\mathbf{P}_r$ and $\mathbf{P}_l$ are known using relation (46). Only relations (46) and (48) are evaluated numerically from the knowledge of the eigenvalues and eigenvectors of the transfer matrix. The number of calculations required to obtain this global matrix does not depend on the number of cells N in the structure as the power of the matrices are easy to calculate from Eq. (46). Calculation of the matrix exponents in Eq. (48) is trivial since, for example, $\mathbf{P}_l^{N} = \mathbf{Q}^{-}\mathbf{\Lambda}^{N}(\mathbf{Q}^{-})^{-1}$, even for fractional N and it involves only the calculation of the powers of the diagonal matrix $\mathbf{\Lambda}$.

Consider a complete structure which is made of several parts i, each part being composed of N_i periodic cells. Fig. 4 presents an example of such a structure made of three parts. Each part is defined from a basic cell repeated N_i times. Using the preceding analysis, the calculation for the whole structure can be done by assembling the dynamic stiffness matrices of each part given by Eq. (48). The main improvement over classical FE methods is that in each set of N_i cells, the usual dynamic stiffness matrix is replaced by a dynamic stiffness matrix with a much smaller number of degrees of freedom. Finally it should be noted that, for a uniform structure, N need not be integral. If the length of the cell is l and that of the uniform region L, then the analysis follows the same lines with $N = L/l$.

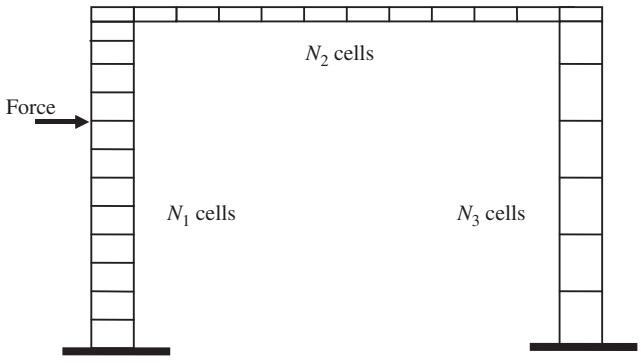

Fig. 4. Structure with three parts made up of periodic structures.

5. Examples

5.1. Beam example

5.1.1. Dynamic stiffness matrix

The beam of length L shown in Fig. 5a, which is fixed on the left side and simply supported on the right side is considered as an example. It is divided into N elements of length l, such that $L = Nl$, and is divided into two regions of lengths $L_1 = N_1 l$ and $L_2 = N_2 l$ by a force F applied at $2/3L$. The beam element with four degrees of freedom is shown in Fig. 5b. This is the basic cell introduced earlier. The elementary stiffness and mass matrices for this element are given by (see for instance Ref. [26])

$$\mathbf{K}_e = \frac{EI}{l^3}\begin{bmatrix} 12 & 6l & -12 & 6l \\ 6l & 4l^2 & -6l & 2l^2 \\ -12 & -6l & 12 & -6l \\ 6l & 2l^2 & -6l & 4l^2 \end{bmatrix}, \quad \mathbf{M}_e = \frac{\rho Sl}{420}\begin{bmatrix} 156 & 22l & 54 & -13l \\ 22l & 4l^2 & 13l & -3l^2 \\ 54 & 13l & 156 & -22l \\ -13l & -3l^2 & -22l & 4l^2 \end{bmatrix}, \tag{49}$$

where E is the Young's modulus, ρ the density of the material, I the second moment of area and S the cross-sectional area. Hysteretic damping is assumed which leads to the damping matrix $\mathbf{C}_e = \eta \mathbf{K}_e$, but the method of analysis can be used for any damping model where the function $\tilde{E}(\mathrm{j}\omega)$ which gives the frequency dependent complex Young's modulus is known. The dynamic stiffness matrix of the element at frequency ω is then $\mathbf{D}_e = \mathbf{K}_e + \mathrm{j}\mathbf{C}_e - \omega^2 \mathbf{M}_e$. It is more convenient to work with non-dimensional quantities, so the displacements are normalised with respect to l and the force and bending moment with respect to $\tilde{E}I/l^2$ and $\tilde{E}I/l$, where $\tilde{E} = (1 + \mathrm{j}\eta)E$. The dynamic stiffness matrix is now

$$\mathbf{D}_e = \begin{bmatrix} 12 - \frac{156}{420}(kl)^2 & 6 - \frac{22}{420}(kl)^2 & -12 - \frac{54}{420}(kl)^2 & 6 + \frac{13}{420}(kl)^2 \\ 6 - \frac{22}{420}(kl)^2 & 4 - \frac{4}{420}(kl)^2 & -6 - \frac{13}{420}(kl)^2 & 2 + \frac{3}{420}(kl)^2 \\ -12 - \frac{54}{420}(kl)^2 & -6 - \frac{13}{420}(kl)^2 & 12 - \frac{156}{420}(kl)^2 & -6 + \frac{22}{420}(kl)^2 \\ 6 + \frac{13}{420}(kl)^2 & 2 + \frac{3}{420}(kl)^2 & -6 + \frac{22}{420}(kl)^2 & 4 - \frac{4}{420}(kl)^2 \end{bmatrix}, \tag{50}$$

where $k = \sqrt{\rho S l^2 \omega^2 / \tilde{E}I}$ is the wavenumber.

5.1.2. Frequency response

The FRF is calculated for excitation by the force F at the position $2/3L$. The forces and the displacements for the parts of the beam on the left and right sides of the force are denoted by the superscript 1 and 2,

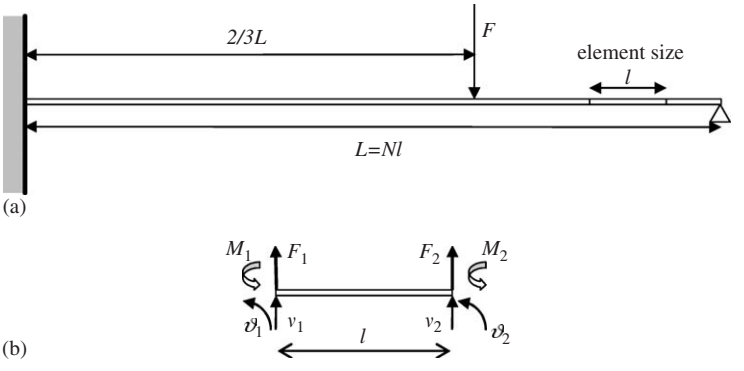

Fig. 5. Beam example: (a) fixed-simply supported beam of length L with force F applied at $2/3L$; (b) single element of the beam.

respectively. They are related by

$$\begin{bmatrix} \mathbf{f}_L^1 \\ \mathbf{f}_R^1 \end{bmatrix} = \mathbf{D}_1 \begin{bmatrix} \mathbf{q}_L^1 \\ \mathbf{q}_R^1 \end{bmatrix},$$
$$\begin{bmatrix} \mathbf{f}_L^2 \\ \mathbf{f}_R^2 \end{bmatrix} = \mathbf{D}_2 \begin{bmatrix} \mathbf{q}_L^2 \\ \mathbf{q}_R^2 \end{bmatrix}, \tag{51}$$

where the matrices $\mathbf{D}_1$ and $\mathbf{D}_2$ are given by Eq. (48) with the propagation matrices calculated from Eq. (50). The following boundary conditions are defined on the left and right sides and at the point where the force is applied:

$$\begin{aligned} &\mathbf{q}_L^1 = 0, \\ &\mathbf{q}_R^1 = \mathbf{q}_L^2, \\ &\mathbf{f}_R^1 + \mathbf{f}_L^2 + \begin{bmatrix} -F \\ 0 \end{bmatrix} = 0, \\ &M_R^2 = 0, \\ &v_R^2 = 0. \end{aligned} \tag{52}$$

Assembling the matrices for the two parts of the beam and eliminating the fixed degrees of freedom gives the global dynamic stiffness matrix. The displacements and rotations can be obtained by solving the system of equations

$$\begin{bmatrix} F \\ 0 \\ 0 \end{bmatrix} = \mathbf{D}_{\text{tot}} \begin{bmatrix} v_L^2 \\ \theta_L^2 \\ \theta_R^2 \end{bmatrix}, \tag{53}$$

where $\mathbf{D}_{\text{tot}}$ is the total dynamic stiffness matrix of the beam. This has now only three degrees of freedom. Fig. 6 shows the theoretical and the numerical predictions for the displacement of the beam per unit input force at the location of the force for a beam with 3, 30, 3000 and 10,000 cells. In this example, the cell is made of steel with $E = 2 \times 10^{11}$ Pa, $\rho = 7800\,\text{kg/m}^3$, $I = 8.33 \times 10^{-14}\,\text{m}^4$, $L = 1\,\text{m}$, $S = 10^{-6}\,\text{m}^2$ and $\eta = 0.01$. The results for three cells are clearly inaccurate except for very low frequencies, showing that the cell size is too large in this case. The calculations for 30 and 3000 cells provide a very good comparison with the analytical solution. Thus the waveguide element approach is accurate for cells with very different scales and is essentially accurate if $kl < 2$. However, the case with 10,000 cells shows the limits of the method when the cell size becomes too small. The solution is no longer accurate for low frequencies. This is not a real problem in practice as the need for very small cells is for high frequency vibration. It should be noted that the computation time is independent of the number of cells, which is a great advantage over classical FE methods.

5.2. Plate example

The example of a simply supported plate excited by a force F in the middle as shown in Fig. 7 is considered. The numerical results are obtained from Ansys stiffness and mass matrices for the mesh of a strip made of 100 elements of type shell63 and size 0.01 m × 0.01 m with four nodes. The material is steel with the same parameters as for the beam. The width is $l = L/100$, which means that $N = 100$ cells are necessary to model the whole plate.

The approach is similar to the beam case except that the dynamic stiffness matrix comes from Ansys. The following boundary conditions are defined on the left and right sides and at the point where the force is applied:

$$\begin{aligned} &\mathbf{q}_L^1, \mathbf{f}_L^1 \text{ simply supported}, \\ &\mathbf{q}_R^1 = \mathbf{q}_L^2, \\ &\mathbf{f}_R^1 + \mathbf{f}_L^2 + \mathbf{F} = 0, \\ &\mathbf{q}_R^2, \mathbf{f}_R^2 \text{ simply supported}. \end{aligned} \tag{54}$$

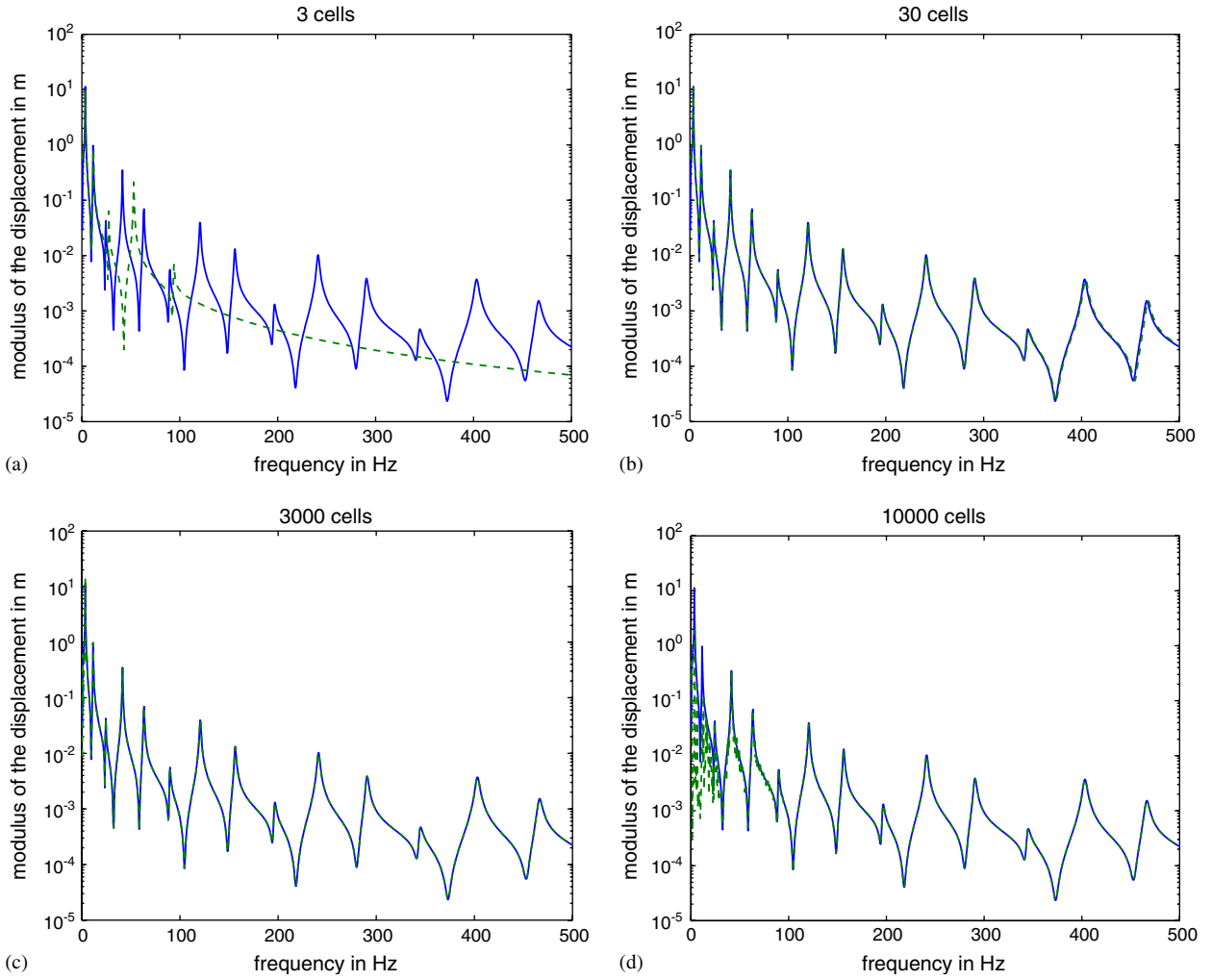

Fig. 6. FRFs of the beam for different numbers of elements calculated using the WFE approach compared with analytical FRFs, — analytical, - - - waveguide: (a) 3 cells; (b) 30 cells; (c) 3000 cells; (d) 10,000 cells.

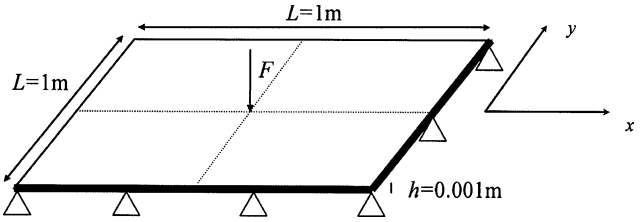

Fig. 7. Simply supported plate excited at the centre.

As the simply supported boundary conditions are not easy to apply in the reduced basis, we propose to write the boundary condition as $\mathbf{Aq} = \mathbf{Cf}$ where $\mathbf{A}$, $\mathbf{C}$ are some matrices, not necessarily invertible and often with many zeros and few 1's as entries. From the relations $\mathbf{q} = \mathbf{Q}^{+}\mathbf{r}$ and $\mathbf{g} = \mathbf{Q}^{+^{\mathrm{T}}}\mathbf{f}$ relating the coordinates of the forces and displacements in the reduced and usual basis, using the approximation

$$\mathbf{f} = \mathbf{Q}^{+}(\mathbf{Q}^{+^{\mathrm{T}}}\mathbf{Q}^{+})^{-1}\mathbf{g}, \tag{55}$$

the boundary condition in the reduced basis can be written as $\mathbf{A}'\mathbf{r} = \mathbf{C}'\mathbf{g}$ with

$$\mathbf{A}' = \mathbf{Q}^{+\mathrm{T}}\mathbf{A}\mathbf{Q}^{+};\ \mathbf{C}' = \mathbf{Q}^{+\mathrm{T}}\mathbf{C}\mathbf{Q}^{+}(\mathbf{Q}^{+\mathrm{T}}\mathbf{Q}^{+})^{-1}. \tag{56}$$

The displacements and rotations can be obtained by the solution of the following system, where $\mathbf{D}_{\mathrm{tot}}$ is the total dynamic stiffness matrix of the plate:

$$\mathbf{G}_{\mathrm{ext}} = \mathbf{D}_{\mathrm{tot}}\mathbf{r}. \tag{57}$$

This can also be written as

$$\begin{bmatrix}\mathbf{g}_1\\ \mathbf{g}_2\\ \mathbf{g}_3\end{bmatrix} = \begin{bmatrix}\mathbf{D}_{11} & \mathbf{D}_{12} & \mathbf{O}\\ \mathbf{D}_{21} & \mathbf{D}_{22} & \mathbf{D}_{23}\\ \mathbf{O} & \mathbf{D}_{32} & \mathbf{D}_{33}\end{bmatrix}\begin{bmatrix}\mathbf{r}_1\\ \mathbf{r}_2\\ \mathbf{r}_3\end{bmatrix} \tag{58}$$

and finally the global system can be written as

$$\begin{bmatrix}\mathbf{0}\\ \mathbf{g}_2\\ \mathbf{0}\end{bmatrix} = \begin{bmatrix}\mathbf{C}'\mathbf{D}_{11} - \mathbf{A}' & \mathbf{C}'\mathbf{D}_{12} & \mathbf{O}\\ \mathbf{D}_{21} & \mathbf{D}_{22} & \mathbf{D}_{23}\\ \mathbf{O} & \mathbf{C}'\mathbf{D}_{32} & \mathbf{C}'\mathbf{D}_{33} - \mathbf{A}'\end{bmatrix}\begin{bmatrix}\mathbf{r}_1\\ \mathbf{r}_2\\ \mathbf{r}_3\end{bmatrix}, \tag{59}$$

with the reduced force component given by $\mathbf{g}_2 = \mathbf{Q}^{+\mathrm{T}}\mathbf{f}_2$.

Fig. 8 shows the displacement of the centre of the plate due to excitation by the force F. Waveguide calculations for different number of modes used to calculate the reduced matrix (11) and the analytical solution are shown. The two results agree very well provided more than 30 modes are used in the calculation. This means that a section can be accurately described with 30 degrees of freedom instead of 299 degrees of freedom which are necessary in the FEM model of a cross section. Fig. 9 compares the analytical solution and the present waveguide solution with Ansys standard modal analysis for 10×10 and 100×100 elements. Clearly a mesh with 10×10 elements is not enough to obtain an accurate solution but the solution with 100×100 elements is much more accurate. The calculation with Ansys requires about 600 Mb of disk space compared to about 6 Mb for the waveguide approach. A similar reduction is obtained in memory requirement.

6. Conclusions

A numerical method for calculating the vibrations of uniform waveguides and periodic structures has been presented. The starting point of this approach is the dynamic stiffness matrix of a cell of the structure, which is

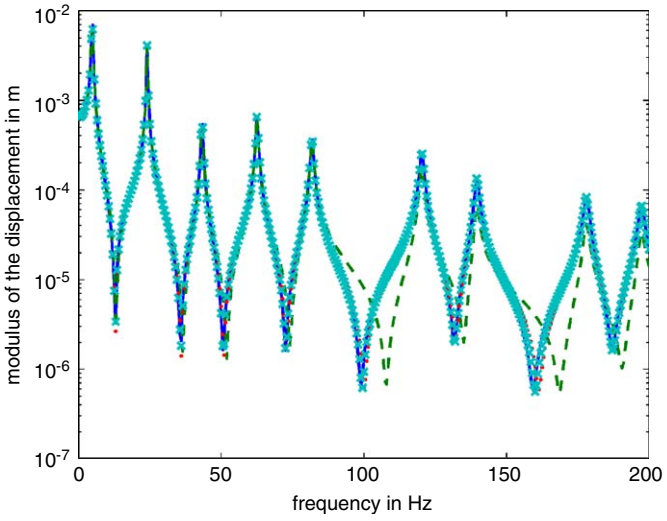

Fig. 8. Comparison of simply supported plate FRFs calculated using analytical and WFE methods, — analytical, - - - waveguide 20 modes, ⋯ waveguide 30 modes, × × × waveguide 40 modes.

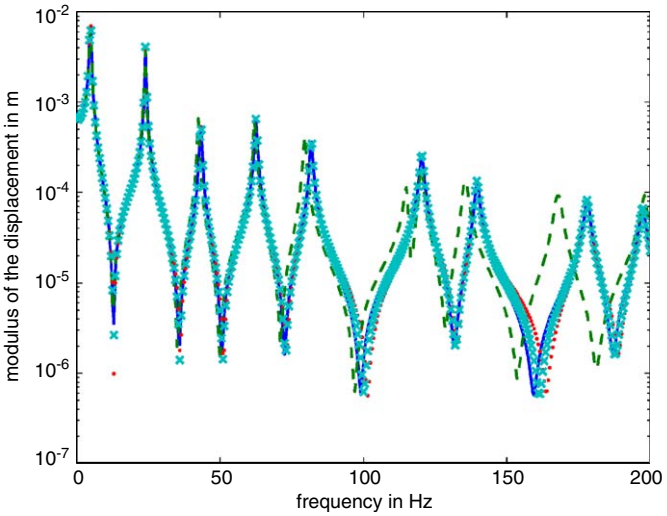

Fig. 9. Comparison of simply supported plate FRFs calculated using analytical, WFE and Ansys modal analysis methods, — analytical, - - - Ansys 10×10 elements, ⋯ Ansys 100×100 elements, $\times \times \times$ waveguide with 30 modes.

obtained from standard FE software after meshing the cell and finding the mass and stiffness matrices. To analyse the structure in terms of waves, the transfer matrix linking the displacements and forces on both sides of a cell was introduced. The propagation constants and the wave basis are the eigenvalues and eigenvectors of the transfer matrix, respectively. This basis allows the decomposition of the state vector, which comprises the displacements and forces in a section, into wave amplitudes. Thus, the behaviour of a structure with N cells can be written in a simple way in terms of wave amplitudes and, after some algebra, the dynamic stiffness matrix of the global structure is obtained. A simple, explicit and stable expression is found for this matrix.

Examples of point force responses for beams and plates show that the accuracy of the present approach is good when the size of the cell is small compared to a wavelength. Compared to standard FE approaches, the cost of a calculation with the WFE approach is reduced because only one cell has to be meshed rather than the whole structure. The other advantage is that standard FE packages can be used to mesh a cell, which cannot be done with the SFE approach, which requires the development of new elements for each application. The model is also valid for any type of damping. The link with Ansys to obtain the stiffness and mass matrices allows more complex structures to be modelled than the examples shown here.

References

[1] D. Wang, C. Zhou, J. Rong, Free and forced vibration of repetitive structures, *International Journal of Solids and Structures* 40 (2003) 5477–5494.
[2] H. von Flotow, Disturbance propagation in structural networks, *Journal of Sound and Vibration* 106 (1986) 433–450.
[3] L.S. Beale, M.L. Accorsi, Power flow in two- and three-dimensional frame structures, *Journal of Sound and Vibration* 185 (1995) 685–702.
[4] S. Finnveden, Finite element techniques for the evaluation of energy flow parameters, *Proceedings of the Novem*, Lyon (keynote paper), 2000.
[5] S. Finnveden, Evaluation of modal density and group velocity by a finite element method, *Journal of Sound and Vibration* 273 (2004) 51–75.
[6] C.M. Nilsson, Waveguide Finite Elements for Thin-Walled Structures, Licentiate Thesis, KTH, Stockholm, 2002.
[7] P.J. Shorter, Wave propagation and damping in linear viscoelastic laminates, *Journal of the Acoustical Society of America* 115 (2004) 1917–1925.
[8] F. Birgersson, Prediction of Random Vibration Using Spectral Methods, PhD Thesis, KTH, TRITA-AVE, Stockholm, 2003, p. 30.
[9] F. Birgersson, S. Finnveden, C.M. Nilsson, A spectral super element for modelling of plate vibration. Part 1: general theory, *Journal of Sound and Vibration* 287 (2005) 297–314.

[10] F. Birgersson, S. Finnveden, A spectral super element for modelling of plate vibration. Part 2: turbulence excitation, *Journal of Sound and Vibration* 287 (2005) 315–328.
[11] L. Gry, Dynamic modelling of railway track based on wave propagation, *Journal of Sound and Vibration* 195 (1996) 477–505.
[12] L. Brillouin, *Wave Propagation in Periodic Structures*, Dover, New York, 1953.
[13] D.J. Mead, Wave propagation in continuous periodic structures: research contributions from Southampton, 1964–1995, *Journal of Sound and Vibration* 190 (1996) 495–524.
[14] D.J. Mead, A general theory of harmonic wave propagation in linear periodic systems with multiple coupling, *Journal of Sound and Vibration* 27 (1973) 235–260.
[15] D.J. Mead, Wave propagation and natural modes in periodic systems: I. Monocoupled systems, *Journal of Sound and Vibration* 40 (1975) 1–18.
[16] D.J. Mead, Wave propagation and natural modes in periodic systems: II. Multicoupled systems with and without damping, *Journal of Sound and Vibration* 40 (1975) 19–39.
[17] L. Houillon, Modélisation Vibratoire des Carrosseries Automobiles en Moyennes et hautes Fréquences, PhD Thesis, Ecole Centrale de Lyon, Décembre, 1999.
[18] L. Houillon, M.N. Ichchouh, L. Jezequel, Wave motion in thin-walled structures, *Journal of Sound and Vibration* 281 (2005) 483–507.
[19] B.R. Mace, D. Duhamel, M.J. Brennan, L. Hinke, Wavenumber prediction using finite element analysis. *Eleventh International Congress on Sound and Vibration*, St. Petersburg, 2004.
[20] B.R. Mace, D. Duhamel, M.J. Brennan, L. Hinke, Finite element prediction of wave motion in structural waveguides, *Journal of the Acoustical Society of America* 117 (2005) 2835–2843.
[21] A. Bocquillet, Méthode Énergétique de Caractérisations Vibroacoustiques des Réseaux Complexes, PhD Thesis, Ecole Centrale de Lyon, février, 2000.
[22] M.M. Ettouney, R.P. Daddazio, N.N. Abboud, Some practical applications of the use of scale independent elements for dynamic analysis of vibrating systems, *Computers and Structures* 65 (1997) 423–432.
[23] L. Gry, C. Gontier, Dynamic modelling of railway track: a periodic model on a generalized beam formulation, *Journal of Sound and Vibration* 199 (1997) 531–558.
[24] R.J. Guyan, Reduction of stiffness and mass matrices, *AIAA Journal* 3 (1965) 380–387.
[25] W.X. Zhong, F.W. Williams, On the direct solution of wave propagation for repetitive structures, *Journal of Sound and Vibration* 181 (1995) 485–501.
[26] M. Petyt, *Introduction to Finite Element Vibration Analysis*, Cambridge University Press, New York, USA, 1990.